Int. J. Electrochem. Sci., 13 **(2018)** 4933 – 4945, doi: 10.20964/2018.05.77

International Journal of
ELECTROCHEMICAL
SCIENCE
www.electrochemsci.org

Electrochemical Sensing Application of Isorhamnetin: Detecting Hg^{2+} as an Example

Li Sun[1], *Buhong Gao*[2], *Weina Jiang*[3], *Li Xu* [1,2,4,*], *Wen Lu* [1], *Shilong Yang*[2], *Dong Jiang*[1], *Jichao Chen*[1], *Huayu Xue*[3], *Jiuzhou Shi*[1]

[1] College of Science, Nanjing Forestry University, Nanjing, 210037, PR China
[2] Advanced Analysis and Testing Center, Nanjing Forestry University, Nanjing, 210037, PR China
[3] College of Chemical Engineering, Nanjing Forestry University, Nanjing, 210037, PR China
[4] China Co-Innovation Center for Sustainable Forestry in Southern China, Nanjing Forestry University, Nanjing, 210037, PR China
[*]E-mail: xuliqby@njfu.edu.cn

Received: 29 January 2018 / *Accepted:* 9 March 2018 / *Published:* 10 April 2018

Isorhamnetin as a natural product has excellent biological activity, but there are few reports of it in electrochemical applications. In this paper, we developed a neoteric electrochemical sensor for sensitive detection of mercury ions (Hg^{2+}) for the first time using glassy carbon (GC) electrode which was modified with isorhamnetin (ISO) and graphene oxide (GO). The electrochemical behaviors of the fabricated GC electrode were characterized by cyclic voltammetry (CV) and differential pulse voltammetry (DPV). Under optimal conditions, the linear range to detect Hg^{2+} with DPV was from 1.0×10^{-6} to 1.0×10^{-4} M with limit detection of 2.3×10^{-8} M (S/N=3). In addition, it also showed excellent selectivity of Hg^{2+} with comparison to several inorganic salt ions and other metal ions. We also report the application for Hg^{2+} detection in real water samples with a good recovery (92.1-104.7%). In conclusion, isorhamnetin can be applied in the electrochemical field successfully with extraordinary results.

Keywords: Isorhamnetin, Graphene oxide, Electrochemical application, Mercury ion

1. INTRODUCTION

Currently, with the development of medical industry, many more kinds of natural products are gaining enough attention from researchers, because they are infinite and have great medicinal value. Flavonoids are typical natural products and their biological activities and application have been researched extensively in various tissues [1-4]. Isorhamnetin (4', 5, 7-trihydroxy-3'-methoxyflavone,

ISO), one of the flavonoid compounds, can be widely found in the fruit of Hippophae rhamnoides L. and the leaf of Ginkgo biloba L [5]. It has two benzene rings linked by an oxygen atom in heterocycle which leads to its good electrical and biological activities. In recent years, many studies have reported the beneficial effects of ISO such as anti-allergic [6], anti-platelet [7, 8], anti-cancer [9, 10], anti-inflammation [11] and anti-oxidation [6, 12]. However, ISO has never been reported as an electrode-modification material for electrochemical application on account of its poor conductivity, especially for heavy metal ions sensing. Therefore, we synthesized a kind of partially oxidized graphene from graphite powder. The obtained graphene oxide (GO) as the oxide product of graphene has good hydrophilicity and great electric conductivity [13-17].

As we all know, heavy metals pollution as one of the environmental problems, is worthy of attention because of its attendant negatives [18]. Among all the heavy metals, Hg^{2+} is a representative and threatening pollutant which can destroy the endocrine and nervous systems of living organisms [19-21]. Additionally, under the condition of microorganisms, inorganic mercury such as metal mercury and Hg^{2+} can be converted into methyl mercury and dimethyl mercury, which are the most toxic [22, 23]. Japan's Minamata disease, one of the eight social pollution nuisances, is a sensation in the world owing to methylmercury poisoning [24, 25]. In this case, we used this as a model for detecting Hg^{2+}.

In the project described herein, it's the first time to develop an electrochemical sensor based on a GCE electrode modified with ISO and GO (ISO/GO/GCE), which is not only sensitive to Hg^{2+}, but also broaden the application of ISO in electrochemistry. During the electrochemical detection process, the redox reaction happened between the free methoxy and phenolic hydroxyl groups of the ISO, as shown in scheme 1 [26].

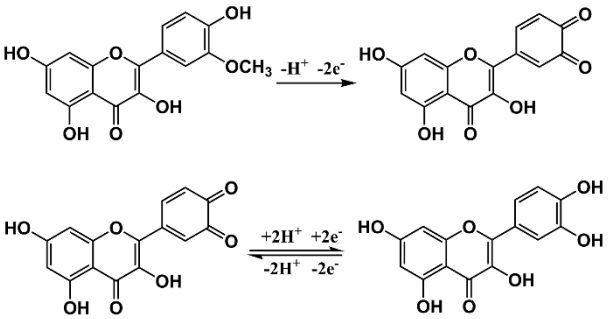

Scheme 1. The reaction mechanism of isorhamnetin at ISO/GO/GCE

2. EXPERIMENTAL

2.1. Materials and reagents

Isorhamnetin was acquired from Aladdin Chemistry Co. Ltd. (Shanghai, China). Natural graphite powder and anhydrous ethanol (CH_3CH_2OH) were offered by Sinopharm Chemical Reagent Co. Ltd. (China). Nitric acid (HNO_3), hydrochloric acid (HCl), sulfuric acid (H_2SO_4) and Potassium

permanganate ($KMnO_4$) were bought from Nanjing Chemical Reagent Co. Ltd. (Nanjing, China). Hydrogen peroxide (H_2O_2) was obtained from Xilong Chemical Co. Ltd. (Shantou, China). All chemicals were of analytical reagent grade. The water used in the experiment was ultrapure water. Real water samples were sourced locally.

2.2 Apparatus

Modified materials were characterized by Fourier Transform Infrared Spectroscopy (FT-IR), Raman Spectroscopy and Transmission Electron Microscopy (TEM). FT-IR spectrum was generated on a Bruker Vertex 80 spectrometer (0.2 cm^{-1}) in the wave number range of 500-4000 cm^{-1}. The Raman data was collected on a Thermo Fisher DXR laser Raman spectrometer. TEM observation was accomplished using a JEOL-2100 apparatus with working voltage of 200 kV. All electrochemical measurements were performed on a CHI660E electrochemistry workstation (Shanghai CH Instruments Inc., China). In the experiment, a three-electrode system was applied with bare and modified glassy carbon electrodes (3 mm in diameter) as working electrodes, respectively. A saturated calomel electrode (SCE) (saturated KCl) and a Pt wire electrode were used as the reference and counter electrodes, respectively. All the experiments were carried out at room temperature.

2.3 Electrode preparation

2.3.1 Preparation of GO/GCE

Partially oxidized graphene was synthesized from graphite powder by a modified Hummers method [27-29] which can keep the water solubility and electrical conductivity of GO. Prior to the modification, the GCE was polished by 0.3 and 0.05 μm α-alumina, and then the GCE was washed by ultrasonification with anhydrous alcohol and ultrapure water successively and at last dried in air.

1 mg GO powder was dispersed into 1 mL ultrapure water by ultrasonification for 30 minutes to form a homogeneous mixture. Then 5 μL of the mixture was carefully cast on the surface of the well-polished GCE and the electrode was allowed to dry at room temperature. In the end, we can get the GO/GCE electrode.

2.3.2 Modification of the GO/GCE surface

5 μL of 1 mg/mL stable Isorhamnetin aqueous solution was dropped on the surface of GO/GCE and the electrode was left in air to evaporate the solvent slowly. The modified GO/GCE with a film of Isorhamnetin named as ISO/GO/GCE was used for detecting Hg^{2+}.

2.4 Electrochemical determination

Before examination, the modified electrodes were deposited at -0.90 V for 250 s. Then they were examined by differential pulse voltammetry (DPV) in 0.01 M phosphate buffer solution (PBS) (pH=5) with 1.0×10^{-5} M Hg^{2+} ranging from 0 to 0.2 V, potential step was 0.004 V, amplitude was 0.05 V, pulse width was 0.05 s, sampling width was 0.0167 s and pulse period was 0.5 s. The experiments were triplicates in the same conditions and the average peak heights were used for construction of the calibration curve. The detection mechanism for Hg^{2+} based on ISO/GO/GC electrode was illustrated in Scheme 2.

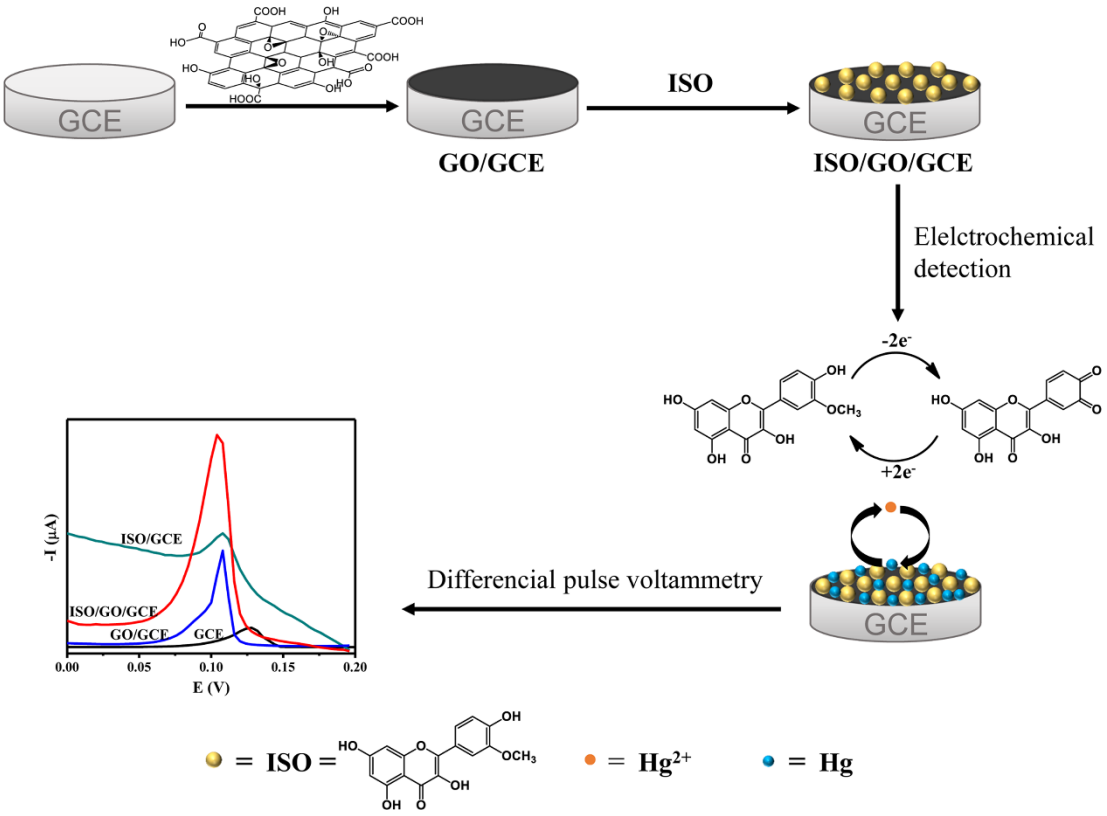

Scheme 2. The fabrication process of the electrochemical sensor and the detection mechanism for the analysis of Hg^{2+}

3. RESULTS AND DISCUSSION

3.1 Materials characterization

The FT-IR experiments as shown in Fig.1A and B were carried out to further characterize the formation of GO and the modification by ISO. Peak at 3434 cm^{-1} of the natural graphite powder (a) is probably due to the existence of little water. GO (b) has numerous oxygen-containing functional groups such as carboxyl, epoxy, hydroxyl [30]. The FT-IR spectrum of the prepared GO reveals the characteristic bands of C=C stretch at 1623 cm^{-1} as well as -OH stretching vibration appearing at 3416

cm^{-1} and C-H bending vibrations at 1402 cm^{-1}. The band around 1726 cm^{-1} corresponds to C=O stretching vibrations from carbonyl and carboxylic groups and the band around 1067 cm^{-1} is attributed to C-O-C stretching vibrations which indicate that GO was synthesized successfully. In the curve of ISO (c), peaks at 3241 cm^{-1} and 1657 cm^{-1} are the results of -OH stretching vibrations and C=O stretching vibrations respectively. Bands around 1615 cm^{-1}, 1561 cm^{-1} and 1512 cm^{-1} are caused by the skeletal vibration of aromatic ring.

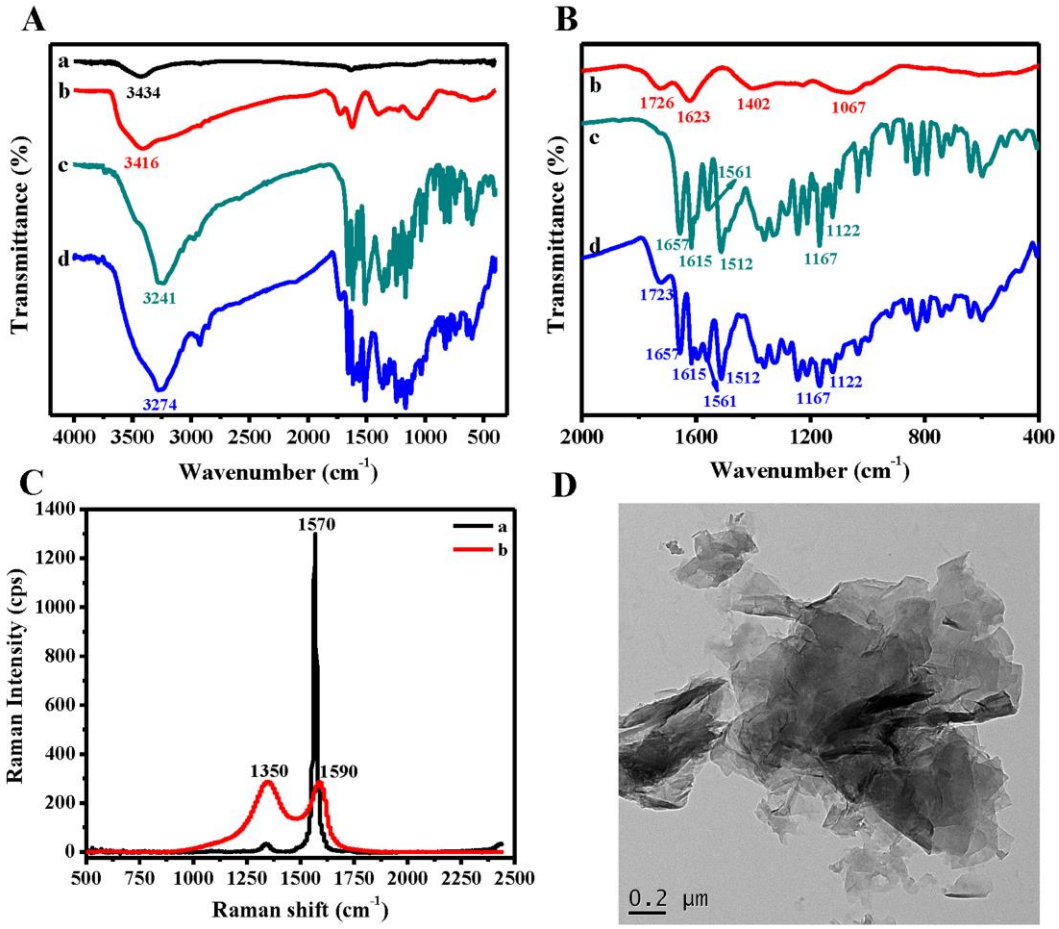

Figure 1. A: The FT-IR spectra of (a) Natural graphite powder, (b) GO, (c) ISO, (d) ISO/GO. B: the partly enlarged FT-IR spectra of A. C: The Raman spectra of (a) Natural graphite powder, (b) GO. D: TEM image of GO.

The asymmetric stretching vibration of C-O-C appears at 1167 cm^{-1} and 1122 cm^{-1}. For all the above, we can ascertain that the structure of ISO is correct. Combining curve b with curve c, the FT-IR spectrum of ISO/GO (d) manifests that the surface of GO/GCE was successfully modified with ISO.

Raman spectroscopy is an effective tool for characterizing the structure and properties of carbon nanomaterials. The G peak in the Raman spectrum of the carbon nanomaterial represents the E_{2g} vibration model of the sp^2 carbon atom, representing the ordered sp^2 bond structure. The D peak represents the defect and amorphous structure at the edge of the graphene. The degree of graphitization of the nanocarbon material is usually evaluated using the ratio of D and G peak intensities (I_D / I_G) [31-

33]. Figure 1C is a typical Raman spectrum of natural graphite powder and GO excited by 532 nm. Both two Raman curves have two typical Raman characteristics, which are located at about 1350 cm^{-1} (D peak) and around 1580 cm^{-1} (G peak). We can see clearly that, the D band of GO is more obvious than natural graphite powder and the I_D/I_G ratio is increased after modification, which is due to the introduction of oxygen-containing groups during the oxidation process, which led to an increase of defect at the edge of GO. As a result, the conversion of natural graphite powder to GO was accomplished.

TEM observation is also a great method to observe the elaborate structure of materials, especially nanometer materials. Figure 1D is a TEM image of GO and the size scale bar is 0.2 μm. It is obvious that GO has layered structure with fold and crispation on the surface.

3.2 Electrochemical characteristics of modified electrodes

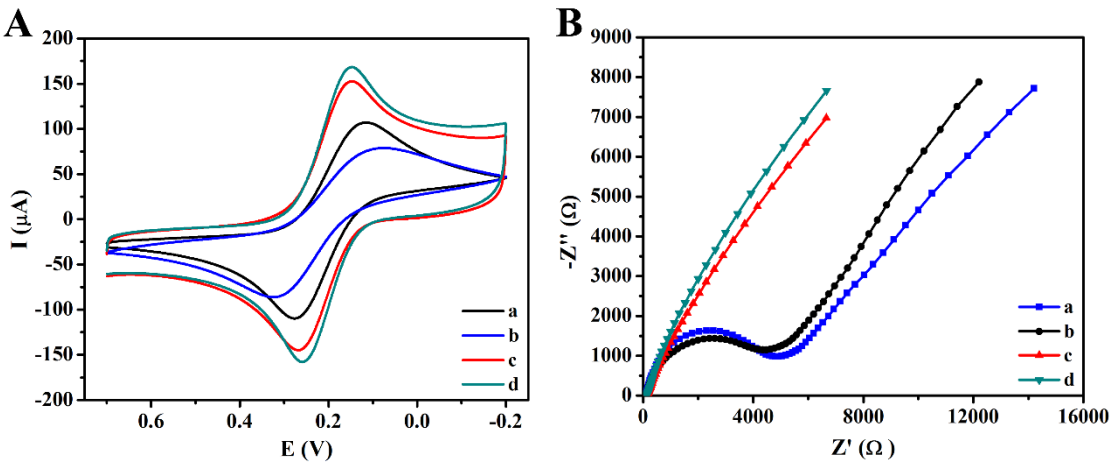

Figure 2. A: Cyclic voltammetry in $[Fe(CN)_6]^{3-/4-}$ solution (5.0 mM containing 0.1 M KCl) at (a) bare GCE, (b) ISO/GCE, (c) ISO/GO/GCE, (d) GO/GCE, scan rate was 0.1 V/s and scan range was from 0.7 V to -0.2 V. B: Electrochemical impedance spectroscopy (EIS) recorded in $[Fe(CN)_6]^{3-/4-}$ solution (1.0 mM containing 0.1 M KCl) at (a) ISO/GCE, (b) bare GCE, (c) ISO/GO/GCE, (d) GO/GCE. Amplitude: 0.005 V. Frequency range: from 0.01 Hz to 0.1 MHz.

Cyclic voltammetry (CV) was applied to probe the surface feature of four treated electrodes. All electrodes were immersed in 5.0 mM $[Fe(CN)_6]^{3-/4-}$ solution containing 0.1 M KCl and depicted by cyclic voltammograms . The scan rate was 0.1 V/s and scan range was from 0.7 V to -0.2 V. As shown in Fig. 2A, a characteristic of diffusion-controlled reversible redox process was observed at bare GCE (a). The redox peak currents prominently increased at GO/GCE (d) demonstrating that GO could accelerate the electron transfer rate effectively. On the contrary, when the surface of bare GCE was modified with Isorhamnetin (b), the peak current decreased obviously due to the poor conductivity of the inert organic natural product. The slight decrease in peak current was seen at ISO/GO/GCE (c) compared with GO/GCE resulting in Isorhamnetin poor conductivity, which indicated the successful modification.

Furthermore, electrochemical impedance spectroscopy (EIS) was carried out in the electrolyte of 1.0 mM $[Fe(CN)_6]^{3-/4-}$ containing 0.1 M KCl. The Nyquist plot of EIS includes two parts, the linear segment at lower frequencies shows a controlled diffusion process and the semicircle part at higher frequencies corresponds to the electron transfer limited process. The diameter of the semicircle represents the electron transfer resistance (R_{ct}). EIS measured results were clearly shown in Fig. 2B. The bare GCE (b) had a semicircle at higher frequencies and the R_{ct} of ISO/GCE (a) was increased caused by the poor conductivity of Isorhamnetin. In addition, we could hardly find the semicircles of ISO/GO/GCE (c) and GO/GCE (d) and their curves were close to straight lines, which indicated that both modified electrodes had excellent conductivity and the R_{ct} was relatively small. However, ISO/GO/GCE had a larger R_{ct} than GO/GCE; this phenomenon showed that Isorhamnetin had poor conductivity than GO and successfully modified the surface of GO/GCE. These results were consistent with the cyclic voltammograms.

3.3 Electrochemical response of Hg^{2+}

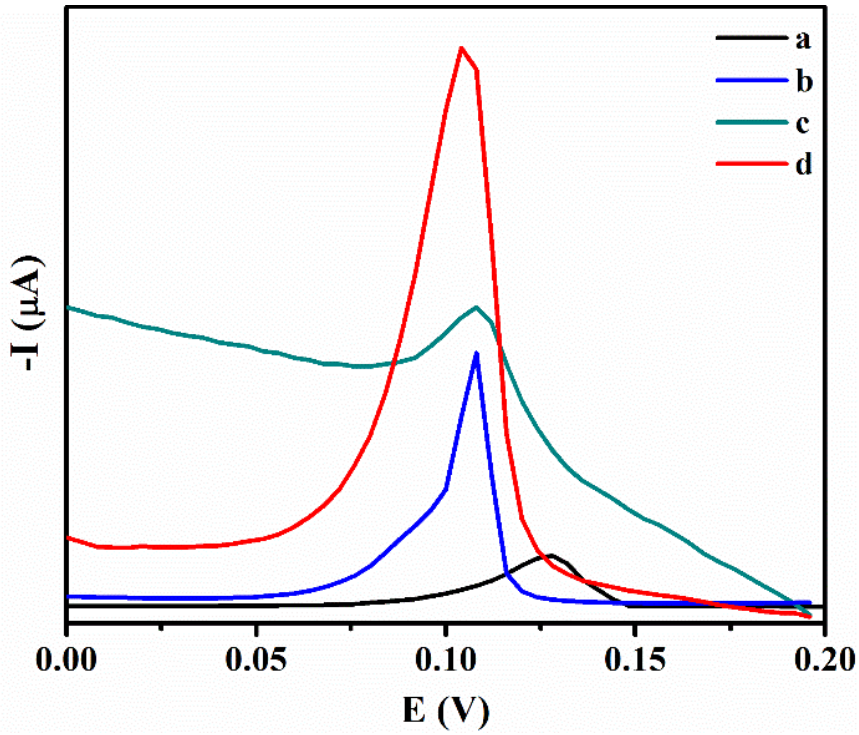

Figure 3. Differential pulse voltammograms (DPVs) of (a) bare GCE, (b) ISO/GCE, (c) GO/GCE, (d) ISO/GO/GCE in 0.01 M phosphate buffer solution (PBS) (pH=5) containing 1.0×10^{-5} M Hg^{2+}. Pulse period: 0.2 s; Amplitude: 0.05 V; Deposition condition: -0.9 V, 250 s.

The electrochemical determination of Hg^{2+} was carried out by deposition at -0.90 V for 250 s before DPV in 0.01 M phosphate buffer solution (PBS) (pH=5) containing 1.0×10^{-5} M Hg^{2+}. Fig.3 illustrated that an excellent oxidation peak at 0.112 V could be found on ISO/GO/GCE (d) and the electrochemical determination signal was distinctly increased compared with the other three electrodes

(a, b, c). These data demonstrated that ISO/GO/GCE could combine with Hg^{2+} effectively and the modified ISO/GO/GCE could be used as a work electrode to detect Hg^{2+}.

3.4 Optimization of experimental variables

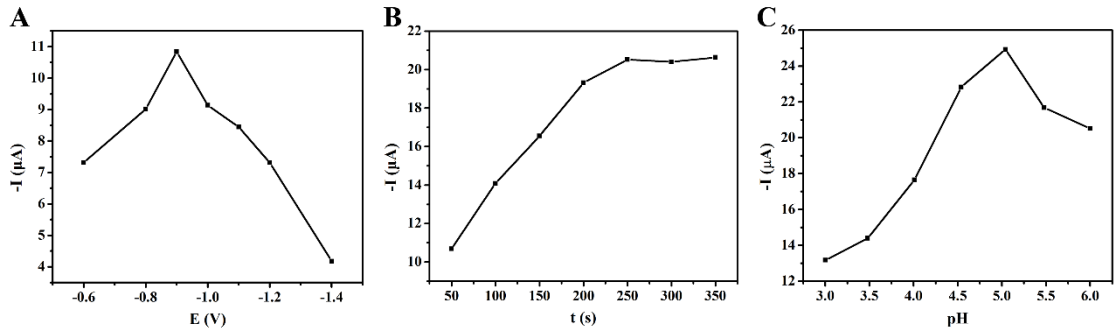

Figure 4. The effect of deposition potential (A), deposition time (B), pH value (C) on the DPV peak current of 1×10^{-5} M Hg^{2+} in 0.01 M PBS at ISO/GO/GCE. Conditions: A: pulse period 0.2 s, amplitude 0.05 V; B: deposition potential -0.90 V, pulse period 0.2 s, amplitude 0.05 V; C: deposition potential -0.90 V, deposition time 250 s, pulse period 0.2 s, amplitude 0.05 V.

Effective deposition benefits the dissolution of Hg^{2+} on the modified electrode surface, which can improve the detection sensitivity and lower the detection limit. Therefore, the effect of deposition potential (range from -0.60 to -1.40 V) was investigated in 0.01 M phosphate buffer solution (PBS) containing 1.0×10^{-5} M Hg^{2+} by DPV with 0.05 V amplitude and scanning potential from 0 to 0.2 V. As can be seen in Fig. 4A, the peak current increased by applying the potential from -0.60 to -0.90 V, and then dramatically decreased from -0.90 to -1.40 V. So, -0.90 V was chosen to be the best deposition potential during the following experiments.

The deposition time plays a significant role in the electrochemical behavior of Hg^{2+}, which is related to the accumulation amount of Hg^{2+} on ISO/GO/GCE surface.

Experiments on the effect of deposition time range from 50 to 350 s were accomplished at the deposition potential of -0.90 V (Fig. 4B), and other measured parameters were the same as in Fig. 4A. It was apparent that the DPV peak current increased gradually from 50 s and tended to be stable until 250 s, showing that 250 s was adequate to reach the saturation of the deposition of Hg^{2+} on the ISO/GO/GCE. There was no doubt that 250 s was selected as the appropriate deposition time.

In addition to the deposition potential and deposition time, the pH value of PBS solution was also an essential parameter to be optimized during electrochemical detection of Hg^{2+}. Fig. 4C showed that the trend of peak current variation increased first and then decreased with pH changing from 3.0 to 6.0 in PBS. It can also be seen that the peak current reached the maximum when pH was about 5.0. Consequently, to enhance detection sensitivity, pH=5.0 of PBS solution was applied to the following experiments.

3.5 Determination of Hg^{2+} based on ISO/GO/GCE electrode

The differential pulse voltammetry is a highly sensitive and a low detection limit electrochemical method, which was used for detecting trace amounts of Hg^{2+} under the optimal conditions. The oxidation currents of different concentrations of Hg^{2+} were obtained in Fig. 5. Fig. 5 showed that there was a good linear relation over the range from 1.0×10^{-6} to 1.0×10^{-4} M. The linear equation was I_p (μA) = -0.0297 + 1.4037 C (μM) with a correlation coefficient of 0.9950. The limit of detection (LOD) was 2.3×10^{-8} M (S/N=3).

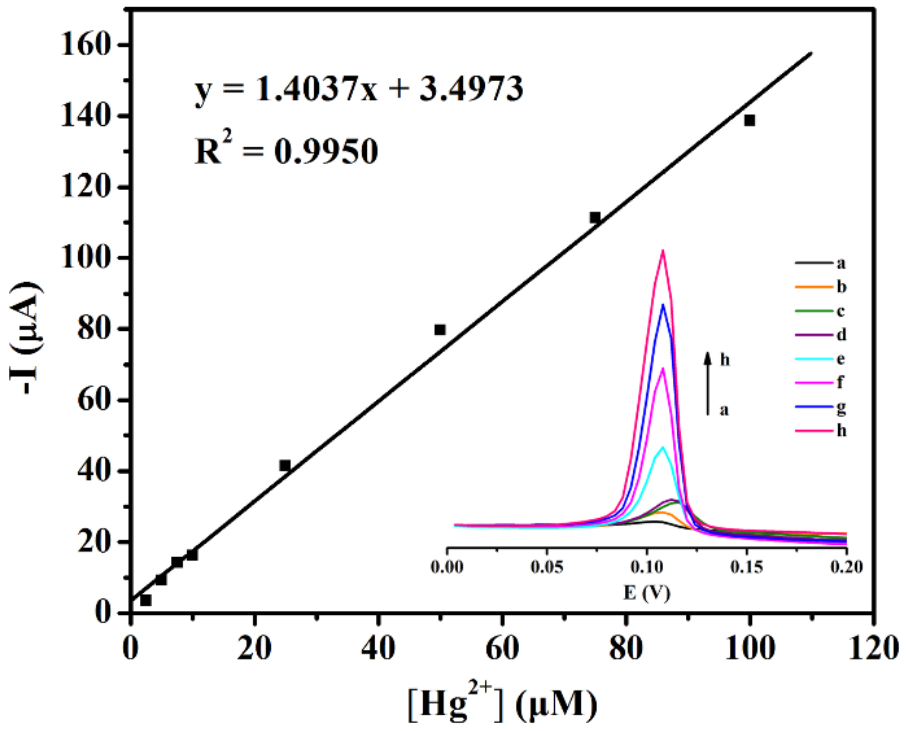

Figure 5. The linear relation between the peak current and concentration of Hg^{2+} at ISO/GO/GCE. Conditions: 0.01 M PBS solution (pH=5.0), deposition potential -0.90 V, deposition time 250 s, pulse period 0.2 s, amplitude 0.05 V. Inset: the corresponding DPV results recording of Hg^{2+} concentrations.

3.6. Interference studies

The influences of possible interferences on the electrochemical response of 1.0×10^{-5} M Hg^{2+} at ISO/GO/GCE was studied by adding some common ions into the same condition. The tolerance limit was defined as the concentration, which gave an error at ≤ 5.0%. From interference experiments of Fig. 6, we can know that 1000 times of Na^+、NO_3^-, 100 times of Mg^{2+}、CH_3COO^-, 50 times of Ca^{2+}、K^+、Cl^-, 10 times of Fe^{3+}、Mn^{2+}、Ni^{2+}, 5 times of Pb^{2+}、Zn^{2+} and 2 times of Al^{3+} don't affect the detection of Hg^{2+}. All the results proved a good selectivity of our sensor. The DPV peak current of six successful modified electrodes under the same conditions was measured to estimate the stability of the sensor. Additionally, the sensor possessed a satisfying stability with the relative standard deviation

(RSD) of only 3.0%. When experiments were performed at the same modified electrode, the RSD of 2.6% demonstrated that the electrochemical sensor exhibited excellent reproducibility.

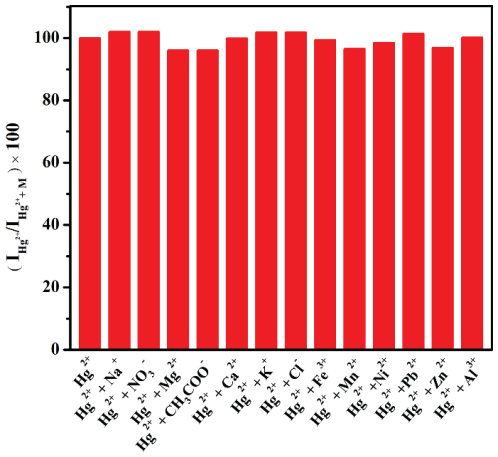

Figure 6. The influences of possible interferences on the electrochemical response of 1.0×10^{-5} M Hg^{2+} at ISO/GO/GCE.

3.7. Real samples analysis

In order to prove the feasibility of practical application, the proposed electrochemical sensor was applied to detecting Hg^{2+} in local water samples including mineral water、tap water、Xuanwu Lake and Qinhuai Lake water. Before the analysis, the four water samples were filtered with 0.22 μm filter membrane and then 0.2 mL of each sample was adjusted to 20 mL PBS solution with known amounts of Hg^{2+}. Two concentration levels of Hg^{2+} with 5 μM and 15 μM were tried using standard addition method. Table 1 listed the percentage of recovery and RSD of spiked Hg^{2+}. The obtained recoveries were in the range of 92.1-104.7% with RSDs of 1.3-5.2%. The satisfactory recoveries of real water samples made the truth that this proposed method can be applied to detect Hg^{2+} in real water samples successfully.

Table 1. The determination of Hg^{2+} in water samples (n=3)

Sample	Added (μM)	Found (μM)	Recovery (%)	RSD (%)
Mineral water	0	ND	-	-
	5.00	4.87	97.4	4.8
	15.00	14.82	98.8	1.5
Tap water	0	ND	-	-
	5.00	4.62	92.4	4.8
	15.00	13.81	92.1	1.3
Xuanwu Lake	0	ND	-	-
	5.00	5.13	102.6	3.5
	15.00	14.67	97.8	5.2
Qinhuai Lake	0	ND	-	-
	5.00	5.21	104.2	2.3
	15.00	15.70	104.7	4.1

ND = Not detected

Table 2. A comparison of the proposed method for the determination of Hg^{2+} with the literature methods.

Electrode/Method	Liner range (μM)	Detection limit (μM)	RSD%	Recovery%	Reference
Colorimetric method with Ag NPs	10-100	2.2	2.2	NA	[34]
Fluorescent chemodosimeter	5.0-200	1.0	2.8-3.0	94.0-97.9	[35]
Nafion-HAP, DPASV	0.1-1.0, 3.0-10	0.03	6.1	94.0-109.0	[36]
BD-NCD, LSV	1.0-10	0.666	NA	NA	[37]
Fe_3O_4, SWASV	1.0-8.0	0.0587	NA	NA	[38]
NiO-CH/GCE, DPV	0.8-500	0.04	8.0	NA	[39]
FFL CuO-CH/GCE, DPV	1.0-200	0.2	3.0	NA	[40]
poly(*p*-ABSA)-SWCNT/GCE, ASV	1.0-500	0.5	1.1-5.8	NA	[41]
ISO/GO/GCE, DPV	1-100	0.023	1.3-5.2	92.1-104.7	This work

NA= Not available

In addition, the proposed method for the determination of Hg^{2+} was compared with the literature methods in Table 2. According to the detection limit, ISO/GO/GCE presents excellent performance compared to other published methods.

4. CONCLUSION

This study is the first time that the application of isorhamnetin in the field of electrochemistry has been expanded. A novel electrochemical sensor was fabricated based on glassy carbon electrode modified with ISO and GO for Hg^{2+} detection. On the base of the optimized deposition potential, deposition time and solution pH, determination of Hg^{2+} with good selectivity, high sensitivity and strong stability was developed. Furthermore, the application of our novel electrochemical sensor for Hg^{2+} detection in real water has achieved great success. Although this approach is only used to detect Hg^{2+}, it can be broadened to the determination of other electroactive substances.

CONFLICTS OF INTEREST

The authors declare no conflict of interest.

ACKNOWLEDGEMENT
This work was financially supported by the National Key Research and Development Program of China (2017YFD0600706), Sate Key Laboratory for Chemistry and Molecular Engineering of Medicinal Resources (Guangxi Normal University) (CMEMR2017-B06), and the priority academic program development of Jiangsu Higher Education Institutions. We also thank Prof. Dr. A. G. Wu (Ningbo Institute of Materials Technology and Engineering, Chinese Academy of Sciences) for his valuable suggestions and help.

References

1. J. Vacek, M. Zatloukalova, T. Desmier, V. Nezhodova, J. Hrbac, M. Kubala, V. Kren, J. Ulrichova and P. Trouillas, *Chem-Biol. Interact*, 205 (2013) 173.
2. T. P. T. Cushnie and A. J. Lamb, *Int. J. Antimicrob. Ag.*, 38 (2011) 99.
3. A. L. Liu, S. B. Zhang, W. Chen, L. Y. Huang, X. H. Lin and X. H. Xia, Talanta, 77 (2008) 314.
4. S. Yang, B. Yin, L. Xu, B. Gao, H. Sun, L. Du, Y. Tang, W. Jiang and F. Cao, *Anal. Methods*, 7 (2015) 4546.
5. G. X. Zhong, J. X. Ye, F. Q. Bai, F. H. Fu, W. Chen, A. L. Liu, X. H. Lin and Y. Z. Chen, *Sensor Actuat. B-Chem.*, 204 (2014) 326.
6. H. Jdir, R. B. Kolsi, S. Zouari, K. Hamden, N. Zouari and N. Fakhfakh, *Lipids Health Dis.*, 16 (2017) 100.
7. A. Perez, S. Gonzalez-Manzano, R. Jimenez, R. Perez-Abud, J. M. Haro, A. Osuna, C. Santos-Buelga, J. Duarte and F. Perez-Vizcaino, *Pharmacol. Res.*, 89 (2014) 11.
8. L. Testai, A. Martelli, M. Cristofaro, M. C. Breschi and V. Calderone, *J. Pharm. Pharmacol.*, 65 (2013) 750.
9. F. Li, W. F. Zhu and F. J. Gonzalez, *Pharmacol. Therapeut.*, 178 (2017) 18.
10. K. A. Manu, M. K. Shanmugam, L. Ramachandran, F. Li, K. S. Siveen, A. Chinnathambi, M. E. Zayed, S. A. Alharbi, F. Arfuso, A. P. Kumar, K. S. Ahn and G. Sethi, *Cancer Lett.*, 363 (2015) 28.
11. J. H. Yang, S. C. Kim, B. Y. Shin, S. H. Jin, M. J. Jo, K. H. Jegal, Y. W. Kim, J. R. Lee, S. K. Ku, I. J. Cho and S. H. Ki, *Food Chem. Toxicol.*, 59 (2013) 362.
12. J. H. Yang, B. Y. Shin, J. Y. Han, M. G. Kim, J. E. Wi, Y. W. Kim, I. J. Cho, S. C. Kim, S. M. Shin and S. H. Ki, *Toxicol. Appl. Pharm.*, 274 (2014) 293.
13. F. N. Xia, D. B. Farmer, Y. M. Lin and P. Avouris, *Nano Lett.*, 10 (2010) 715.
14. D. Li, M. B. Muller, S. Gilje, R. B. Kaner and G. G. Wallace, *Nat. Nanotechnol.*, 3 (2008) 101.
15. A. K. Geim and K. S. Novoselov, *Nat. Mater.*, 6 (2007) 183.
16. M. Pumera, *Electrochem. Commun.*, 36 (2013) 14.
17. K. Zhang, G. Song, L. Yang, J. Zhou and B. Ye, *Anal. Methods*, 4 (2012) 4257.
18. M. Schrope, *Nature*, 409 (2001) 124.
19. J. L. Zhang, Z. W. Zhu, J. W. Di, Y. M. Long, W. F. Li and Y. F. Tu, *Electrochim. Acta*, 186 (2015) 192.
20. P. B. Tchounwou, W. K. Ayensu, N. Ninashvili and D. Sutton, *Environ. Toxicol.*, 18 (2003) 149.
21. S. Amiri, A. Navaee, A. Salimi and R. Ahmadi, *Electrochem. Commun.*, 78 (2017) 21.
22. M. Korolczuk and I. Rutyna, *Electrochem. Commun.*, 10 (2008) 1024.
23. S. Carneado, R. Peró-Gascón, C. Ibáñez-Palomino, J. F. López-Sánchez and A. Sahuquillo, *Anal.Methods*, 7 (2015) 2699.
24. M. Harada, *Crit. Rev. Toxicol.*, 25 (1995) 1.
25. S. J. Balogh, M. T. K. Tsui, J. D. Blum, A. Matsuyama, G. E. Woerndle, S. Yano and A. Tada, *Environ. Sci. Technol.*, 49 (2015) 5399.
26. J. J. Wu, L. Wang, Q. Q. Wang, L. N. Zou and B. X. Ye, *Talanta*, 150 (2016) 61.

27. W. S. Hummers and R. E. Offeman, *J. Am. Chem. Soc.*, 80 (1958) 1339.
28. S. F. Hou, S. J. Su, M. L. Kasner, P. Shah, K. Patel and C. J. Madarang, *Chem. Phys. Lett.*, 501 (2010) 68.
29. A. P. Tuan, B. C. Choi, K. T. Lim and Y. T. Jeong, *Appl. Surf. Sci.*, 257 (2011) 3350.
30. J. B. Li, X. J. Wang, H. M. Duan, Y. H. Wang, Y. N. Bu and C. N. Luo, *Talanta*, 147 (2016) 169.
31. P. G. Ren, D. X. Yan, X. Ji, T. Chen and Z. M. Li, *Nanotechnology*, 22 (2011) 55705.
32. B. Li, L. Zhou, D. Wu, H. L. Peng, K. Yan, Y. Zhou and Z. F. Liu, *Acs Nano*, 5 (2011) 5957.
33. S. Bong, Y. R. Kim, I. Kim, S. Woo, S. Uhm, J. Lee and H. Kim, *Electrochem. Commun.*, 12 (2010) 129.
34. K. Farhadi, M. Forough, R. Molaei, S. Hajizadeh and A. Rafipour, *Sensor Actuat. B-Chem.*, 161 (2012) 880.
35. X. Zhang and Y. Y. Zhu, *Sensor Actuat. B-Chem.*, 202 (2014) 609.
36. F. Gao, N. N. Gao, A. Nishitani and H. Tanaka, *J. Electroanal. Chem.*, 775 (2016) 212.
37. E. Nurhayati, Y. J. Juang, M. Rajkumar, C. Huang and C. C. Hu, *Sep. Purif. Technol.*, 156 (2015) 1047.
38. W. J. Li, X. Z. Yao, Z. Guo, J. H. Liu and X. J. Huang, *J. Electroanal. Chem.*, 749 (2015) 75.
39. Z. C. Wu, L. D. Jiang, Y. A. Zhu, C. R. Xu, Y. Ye and X. H. Wang, *J. Solid State Electr.*, 16 (2012) 3171.
40. Z. C. Wu, L. D. Jiang, H. M. Chen, C. R. Xu and X. H. Wang, *J. Mater. Sci-Mater. El.*, 23 (2012) 858.
41. J. Lv, Y. Tang, L. M. Teng, D. Y. Tang and J. Zhang, *J. Serb. Chem. Soc.*, 82 (2017) 73.